

The Formation of One-Lobed Stokes V Profiles in an Inhomogeneous Atmosphere

S. R. O. Ploner, M. Schüssler, S. K. Solanki

Max-Planck-Institut für Aeronomie, D-37191 Katlenburg-Lindau, Germany

V. A. Sheminova, A. S. Gadun

Main Astronomical Observatory of Ukrainian NAS, Goloseevo, 252650 Kiev-22, Ukraine

C. Frutiger

Institute of Astronomy, ETH-Zentrum, CH-8092 Zürich, Switzerland

Abstract. We assess the diagnostic potential of the observed ‘pathological’ Stokes V profiles that differ strongly from the customary, nearly antisymmetric two-lobed shape. In particular, we consider the formation of one-lobed Stokes V profiles using the results of an MHD simulation. We find that the majority of one-lobed profiles is produced in regions of weak horizontal field with significant cancellation caused by mixed polarity along the line of sight. A minority of one-lobed profiles originates close to strong magnetic field concentrations with strong gradients of velocity and magnetic field strength.

1. Introduction

Polarization measurements of photospheric spectral lines are widely used to infer the properties of the magnetic and velocity fields in the solar atmosphere. Owing to the finite width of the contribution function, such information is encoded in the Stokes profiles in a strongly convoluted form, particularly if significant gradients of magnetic field and velocity along the line of sight (LOS) lead to ‘abnormal’ (see below) Stokes profiles. Under such circumstances the inversion problem, i.e., the interpretation of the Stokes profiles in terms of the physical properties of the atmosphere becomes very difficult.

‘Normal’ V profiles possess two lobes having amplitudes of opposite sign. Profiles which strongly deviate from this shape are called ‘abnormal’; such profiles are present in observations (e.g. Rüedi et al. 1992). A particular class of abnormal profiles are one-lobed (OL) profiles which essentially consist of one lobe while the other is not present or very small. OL profiles are by no means rare exceptions: Sigwarth et al. (1999) report an occurrence of 3% in active regions. Since OL profiles can be viewed as extremely asymmetric profiles, gradients of the LOS component of both magnetic field and velocity have to exist

(e.g. Solanki 1993). Therefore OL profiles may contain important information about the structure of magnetic elements.

In order to better understand the origin of OL profiles, a forward approach is commonly used, i.e. synthetic profiles are determined using empirical or other postulated model atmospheres. Rüedi et al. (1992) generate highly asymmetric Stokes V profiles by assuming that two magnetic components of opposite polarity are present within the spatial resolution element. Sánchez Almeida et al. (1996) introduce the concept of magnetic micro-structuring (MISMA) by means of a statistical ensemble of optically thin magnetic elements along the LOS. This allows them to reproduce – among other kinds of abnormal profiles – extremely asymmetric Stokes V profiles. Grossmann-Doerth et al. (2000) investigate the influence of interfaces onto Stokes profiles. Their first example corresponds to the magnetopause of an upward expanding magnetic flux tube in which the ray passes through magnetized plasma at rest and then through moving field-free plasma. In the second example, a vertical ray intersects an inclined flux tube harboring a flow. Both configurations lead to the formation of OL profiles. Recently, Steiner (2000) suggested that a suitable change of temperature across a magnetopause can give rise to various kinds of abnormal Stokes V profiles, including the OL profiles.

As the above mentioned authors present different possible formation scenarios of OL profiles, the question of the relative importance of these mechanisms arises. The question whether other scenarios also lead to OL profiles remains open. In order to address these questions we take a different approach and synthesize profiles using the output of a MHD simulation. This approach has the advantage that such model atmospheres are physically consistent solutions of the MHD equations and that we do not prescribe a scenario producing OL profiles, but search within the output of the code for the physical conditions that give rise to OL profiles.

2. Calculation and selection of Stokes profiles

The calculation of the synthetic Stokes profiles is based on atmospheres resulting from the MHD simulation described in these proceedings by Ploner et al. (2001). We take 120 snapshots covering one hour of solar time. Each snapshot is covered by 200 equidistant vertical rays (lines of sight, LOS). The Stokes profiles are determined for the line Fe I 6302.5 Å and correspond to a hypothetical observation at disc center.

In order to isolate OL profiles we determine all local extrema of the V profiles and then consider as significant only those extrema which exceed 10% of the magnitude of the largest extremum. We define as OL profiles those which have only one significant extremum. Note that this criterion selects profiles with an amplitude asymmetry, δa (cf. Solanki 1993), larger than 82%.

We find that 45.5% (10,686) of all profiles are abnormal and that 3.6% (379) of these are OL, which is in good agreement with the results of Sigwarth et al. (1999). Figure 1 shows the spatio-temporal distribution of the OL profiles (indicated by circles) upon a grey scale image displaying the vertical magnetic field component. Only few OL profiles are found within magnetic flux concentrations (indicated by lighter and darker than average shading), or lie close to

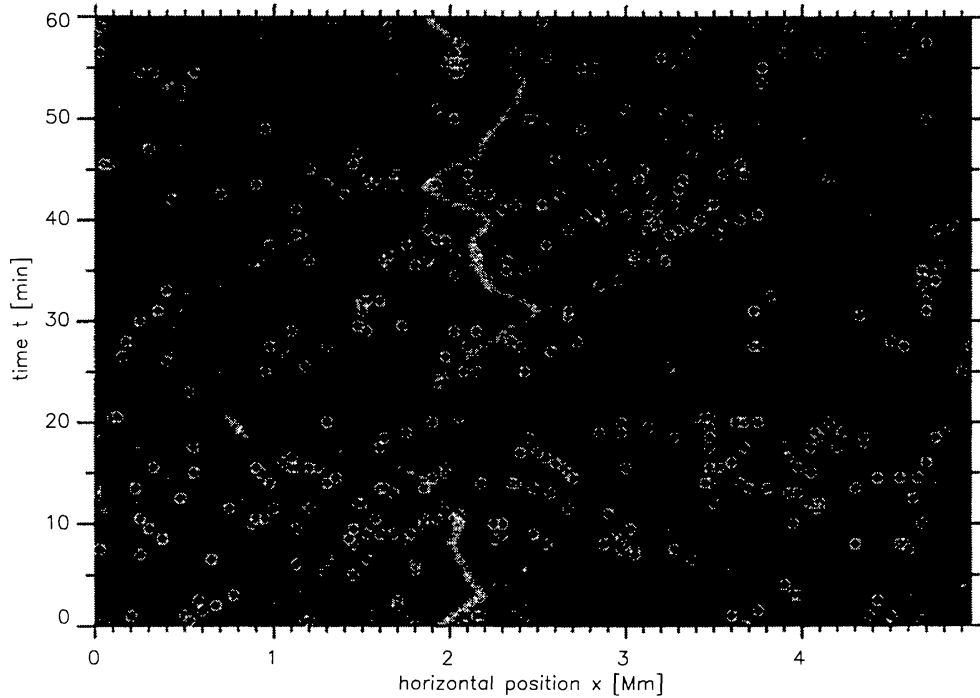


Figure 1. Spatio-temporal distribution of one-lobed (OL) Stokes V profiles (circles) drawn upon a grey-scale image of the vertical magnetic field component. Horizontal position is displayed along the x -axis and time increases from bottom to top along the y -axis. The vertical magnetic field is taken at $\tau = 1$ (τ is the continuum optical depth at $\lambda = 5000\text{\AA}$) with light and dark indicating the two polarities, grey signifies weak vertical field.

such concentrations (e.g. $x = 1.9$ Mm and $t = 44$ min). Most OL profiles are found in regions of weak vertical magnetic field (grey).

3. Results

3.1. One-lobed profiles near flux concentrations

Figure 2 shows an example of a OL profile (see lower right edge) together with its formation along the LOS. In the case shown here, the profile is mainly formed around $\log(\tau) = -0.6$ and is built up by contributions which are strongly asymmetric owing to the strong gradients of field strength and velocity. The broad red wing is caused by the integration of contributions with varying Doppler shift. Figure 3 shows a snapshot of part of the computational domain containing the LOS that corresponds to Fig. 2 (indicated by the thick vertical line). The origin of the large magnetic field and velocity gradient along the LOS is the formation of a kink in a magnetic field concentration.

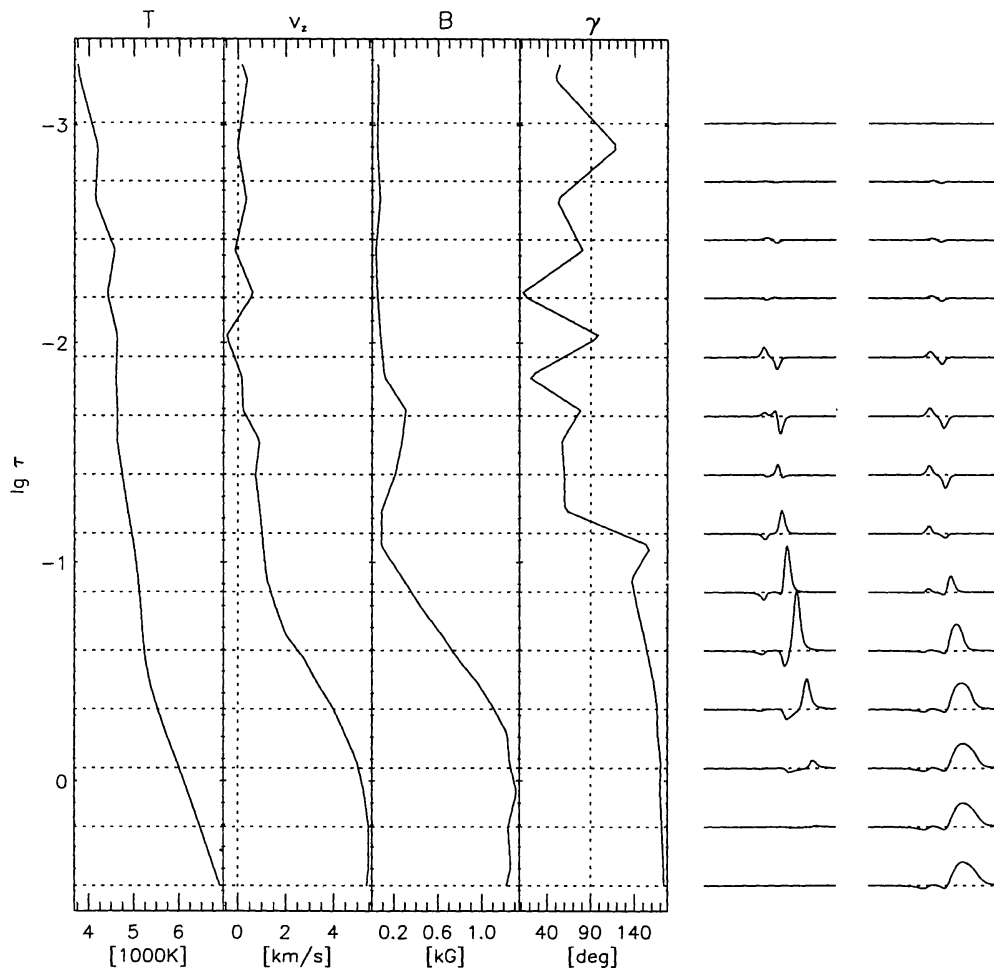


Figure 2. Atmosphere and contributions for an example of a one-lobed profile (the emergent profile is plotted at the lower right edge). The dependence of temperature, T , LOS velocity, v_z , magnetic field strength, B , and field inclination, γ , (horizontal axes) versus optical depth along the LOS, $\log(\tau)$ (vertical axis), is displayed (first to 4th column, from left to right). The profiles in the 5th column correspond to the line depression contribution functions (LDF, Grossmann-Doerth et al. 1988) plotted versus wavelength at the depth marked by the horizontal dotted lines in the atmosphere. We call this representation of the LDF contribution *profile* (CP) at a given depth. The profiles in the right column are CP s integrated from above to the indicated depth, i.e. $ICP(\tau) = \int_{\tau}^0 d\tau_0 CP(\tau_0, \lambda)$. This integration path refers to the numerical solution of the radiative-transfer equations.

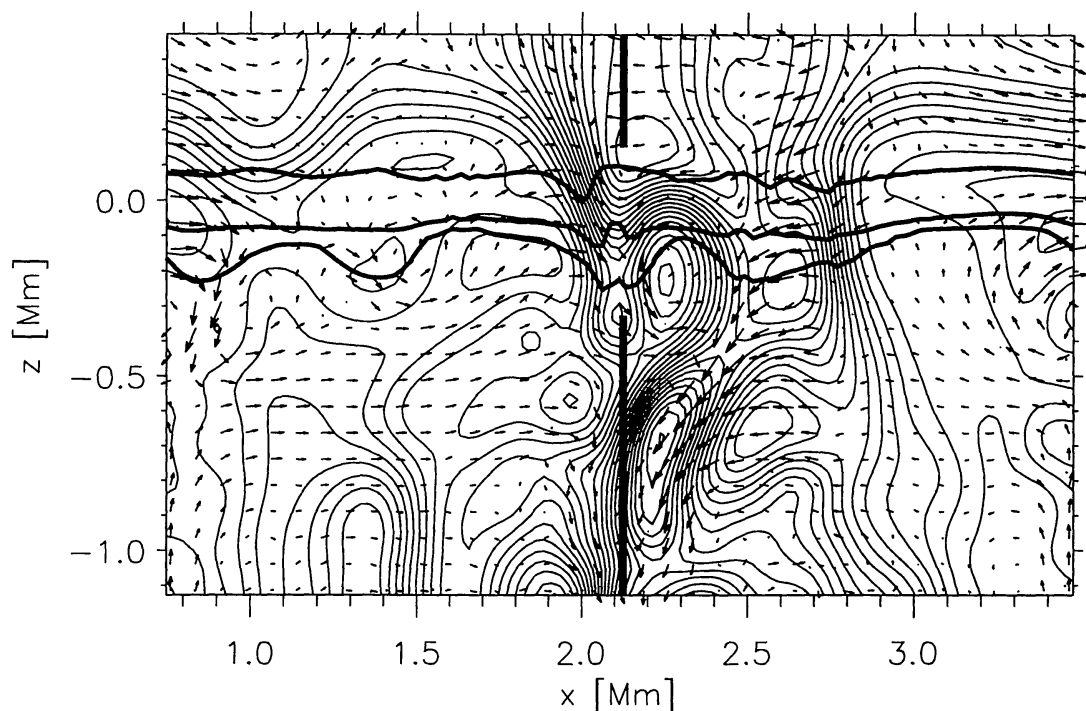


Figure 3. Spatial location of the line of sight (thick vertical line) corresponding to the V profile shown in Fig. 2. Magnetic field lines and velocity arrows are shown in part of the computational domain. The thick horizontal lines indicate the level $\log(\tau) = -1, 0$ and 1 from top to bottom, respectively.

Typical for this kind of OL profile formation is the following: the profile is build up mainly by a single pronounced maximum of the contributions and the maximums' width covers a considerable fraction of the LOS. The contributions are OL due to gradients in magnetic field and velocity belonging to a magnetic interface. This formation scenario, however, applies only to a minority of OL profiles, namely those originating close to magnetic field concentrations.

3.2. One-lobed profiles forming in regions of weak magnetic field

Figure 4 shows an example of a OL profile formed in weak magnetic field. In contrast to the example of Fig. 2, the contributions to this profile peak at several locations along the LOS (around $\log(\tau) = -2.3, -1.8, -1.0$ and -0.5) having there CP with similar magnitude. The integrated contribution profiles, however, remain small in amplitude due to cancellation caused by changes of the polarity along the LOS to which Stokes V is sensitive.

OL profiles from weak-field regions typically have small integrated contributions over a considerable part of the LOS. This can either result from intrinsic

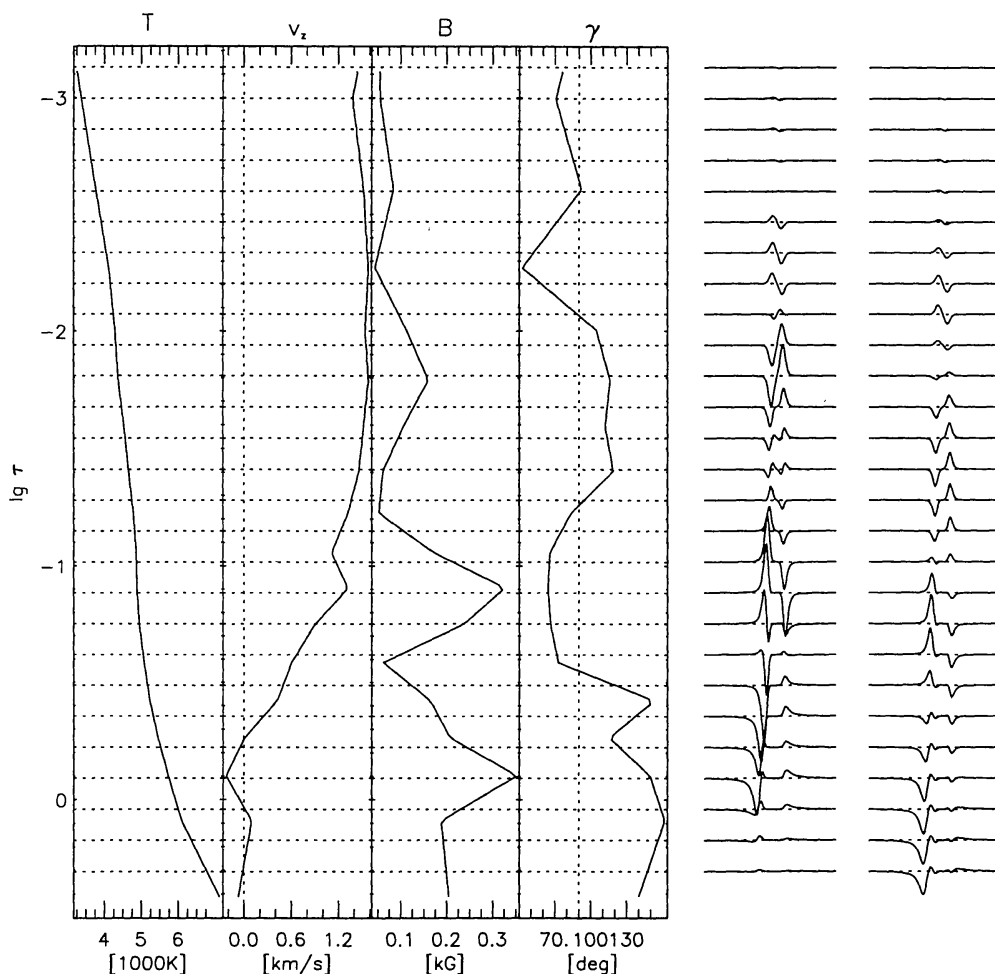


Figure 4. The same as Fig. 3 but for a OL profile formed in weak magnetic field.

sically small contributions (very small LOS component of the magnetic field) or from cancellation of contributions due to polarity changes along the LOS. As a consequence, localized contributions may dominate the resulting V profile. An example of the latter situation is shown in Fig. 4: The contributions above $\log(\tau) = -0.4$ nearly cancel and the final OL profile is formed by the gradients of the LOS magnetic field and velocity below that level, although these contributions per se do not dominate along the LOS. In contrast to the example shown in Fig. 2, the variation of the LOS component of the magnetic field is mainly due to a change in field inclination and not so much to a gradient of its magnitude (like at a magnetic interface).

The histogram plots of Fig. 5 show that the formation scenario described above indeed governs the formation of most OL profiles. The panel on the left side shows that most OL profiles are formed on average in regions of mainly

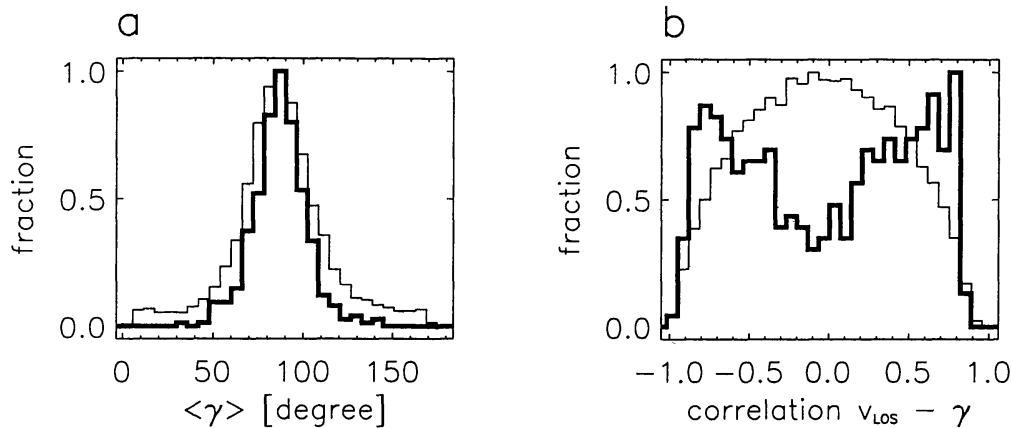


Figure 5. Normalized histograms of the averaged field inclination (frame a) and correlation between LOS velocity, v_{LOS} , and magnetic field inclination, γ (frame b). The field inclination, γ , has been averaged over those parts of the LOS where the wavelength integrated contribution $CP(\tau) = \max_{\lambda}(|CP(\tau, \lambda)|)$ exceeds 1% of its maximum value. Thick lines refer to OL, thin lines to all V profiles.

horizontal magnetic field. The decisive role played by the combination of gradients in LOS velocity and field inclination is indirectly demonstrated by the high correlation along the LOS of these quantities (Fig. 5b) for OL profiles. Note that for OL profiles several polarity reversals are present (not displayed) along the LOS which do not only give rise to cancellation but also to gradients in the field inclination. Such a correlation separates OL profiles from the average behavior of (all) V profiles.

Since the contributions above $\log(\tau) = -0.4$ are more or less symmetrical and cancel each other the profile of Fig. 4 is almost completely formed around the layer $\log(\tau) = -0.5$. We mention that no rule is present that the OL profiles preferentially are formed in a particular layer. Many examples are present in which the contributions are OL at all local maximum of the contributions and since different combinations lead to cancellation no unique location of profile formation can be found.

4. Discussion and Conclusions

We find that 3.6% of all abnormal profiles are one-lobed (OL) profiles. Two major formation mechanisms are found to be present which extend already existing formation scenarios. The first mechanism is characterized by one distinct gradient preferentially towards high velocity and magnetic field strength with increasing depth. The contributions around the location of strong gradients are OL and clearly build up the resulting OL profile. Since this formation mechanism generates the few OL profiles originating close to strong magnetic field concentrations, it resembles the models proposed by Grossmann-Doerth et al. (2000). The mechanism differs from the model of Rüedi et al. (1992), who assume horizontally separated spatially unresolved components whereas the OL

profiles discussed here are the result of an atmospheric structure along the line of sight (LOS).

The second process – responsible for the formation of the major fraction of the OL Stokes V profiles – relies on multiple polarity reversals along the LOS. Such sign changes are easily produced for vertical LOS by a nearly horizontal magnetic field which varies its inclination. The MISMA model of Sánchez Almeida et al. (1996) also includes multiple polarity reversals. The origin of their OL V profiles, lies in the numerous transitions between magnetized and unmagnetized plasma along the LOS and is therefore similar to the our weak-field formation scenario. None of the OL profiles analyzed by us is caused by a temperature reversal as suggested by Steiner (2000). The temperature reversals that are present in the simulation do not lead to OL profiles.

This investigation shows that the diagnostic potential of OL profiles is reduced, since a particular OL profile *alone* does not allow us to differentiate between the two mechanisms. An extension of the present analysis will decide whether the inclusion of additional information may help to differentiate among the two formation mechanisms. On the one hand the relation of the OL V profile to its corresponding Q profile must be considered. On the other hand the behavior of the spatial neighbors of the OL profile may be of interest, particularly if OL V profiles cluster around a certain spatial location or a continuation to asymmetric profiles is present.

References

- Grossmann-Doerth U., Larsson B., Solanki S.K. 1988, *A&A*, 204, 266
 Grossmann-Doerth U., Schüssler M., Sigwarth M., Steiner O. 2000, *A&A*, 357, 351
 Ploner S.R.O., Schüssler M., Solanki S.K., Gadun A.S. 2001, in M. Sigwarth (ed.), *Advanced Solar Polarimetry - Theory, Observation, and Instrumentation*, in press, Asp Conference Series
 Rüedi I., Solanki S.K., Livingston W., Stenflo J.O. 1992, *A&A*, 263, 323
 Sánchez Almeida J., Landi degl' Innocenti E., Martínez Pillet V., Lites B.W. 1996, *ApJ*, 466, 537
 Sigwarth M., Balasubramaniam K.S., Knölker M., Schmidt W. 1999, *A&A*, 349, 941
 Solanki S.K. 1993, *Space Sci. Rev.*, 63, 1
 Steiner O. 2000, *Sol. Phys.*, 196, 245